

Beating Heart Motion Prediction for Robust Visual Tracking

Rogério Richa*, Antônio P. L. Bó, Philippe Pognet
LIRMM - UMR 5506 CNRS - UM 2
161, rue Ada, 34392 Montpellier Cedex 5 - France
firstname.lastname@lirmm.fr

Abstract—In the context of minimally invasive cardiac surgery, robotic assistance has significantly helped surgeons to overcome difficulties related to the minimally invasive procedure. Recently, techniques have been proposed for active canceling the beating heart motion for improving the accuracy of the surgical gestures. In this scenario, computer vision techniques can be applied for estimating the heart motion based solely on natural structures on the heart surface. However, visual tracking is complicated by the particular lighting conditions and clutter (smoke, liquids, etc) during surgery. Another challenging problem are the occasional occlusions by surgical instruments. In order to overcome these problems, we exploit the quasi-periodicity of the beating heart motion for increasing the robustness of the visual tracking task. In this paper, a novel time-varying dual Fourier series for modeling the quasi-periodic beating heart motion is proposed. For estimating the series parameters, an Extended Kalman Filter (EKF) is used. The proposed method is applied in a visual tracking task for bridging tracking disturbances and automatically reestablish tracking in cases of occlusions. The efficiency of the prediction method and the sensible improvements in the visual tracking task are demonstrated through *in vivo* experiments.

I. INTRODUCTION

Physiological motion considerably disturbs the precise execution of surgical procedures, prolonging the operating time and increasing costs. In minimally invasive surgery (MIS), interventions on a beating heart are made possible by the use of mechanical heart stabilizers. However, considerable residual motion due to insufficient immobilization exists and has to be manually compensated by the surgeon. In this context, robotic assistance could aid surgeons by actively compensating the beating heart motion, potentially improving the precision of their gestures. The idea behind active physiological motion compensation is having the surgical instruments track the heart motion, allowing for surgeons to perform their gestures in a virtually stable operating site.

A motion compensation system depends fundamentally on the accurate retrieval of the heart motion. For this purpose, tracking the heart using the visual feedback provided by the laparoscope is the most practical solution. In the literature, several techniques for tracking the 3D motion of natural landmarks on the heart surface have been proposed [10], [12]. However, these techniques do not take into consideration the heart motion in time and lack robustness when facing the complex heart dynamics, lighting conditions and appearance changes. To cope with these issues, we exploit the quasi-periodicity of the beating heart motion and predict

its future motion using a predictive Extended Kalman Filter (EKF) based on a time-varying dual Fourier series. The goal is to bridge tracking failures and reestablish tracking in case of occlusions (e.g. when the operating site is occluded by surgical tools, smoke, blood etc). The clinical value of the proposed method is demonstrated through *in vivo* experiments, which attest the sensible improvements in the visual tracking task.

A. Background

The heart motion modeling and prediction is also useful in several levels of a surgical robotic assistant design. Notably, the error feedback alone is insufficient for controlling a robotic actuator with a sufficiently low tracking error [3]. In the literature, various paradigms for predicting future positions of a point of interest (POI) on the heart surface have been proposed. In Franke et al. [6], a generalized linear predictor was designed for providing future position estimates of a POI in a robot tracking task. Similarly, Bebek et al. [2] used a copy of the previous heartbeat cycle synchronized with an electrocardiogram (ECG) signal for predicting the following heartbeat cycle. For tracking features on the beating heart using vision, Ortmaier et al. [8] uses embedded vectors of previous heart cycles for increasing tracking resilience. A thorough investigation of the heart motion was performed by Cuvillon [4], who proposed a motion prediction algorithm based on a Linear Parameter Variant model that is a function of the ECG and respiratory signals.

An alternative paradigm also found in the literature for describing the quasi-periodic heart motion is the Fourier series model and different approaches for estimating its coefficients exist. In Ginhoux et al. [7] a known and steady cardiac rhythm is assumed, whereas Thakral et al. [13] proposed the estimation of a non-stationary Fourier series coefficients using Least Mean Squares. A similar approach has also been proposed by Yuen et al. [14] for tracking the Mitral valve annulus motion on a single axis. However, in the methods above, the respiratory and cardiac motions that comprise the heartbeat are treated separately or only the cardiac motion is modeled. Alternative approaches have also been proposed, such as the membrane model presented in Bader et al. [1] and the motion model based on a combination of several basis functions proposed by Duindam et al [5], but experiments using real heart motion are not presented.

In our previous work [9], we introduced an estimation framework based on the Extended Kalman Filter (EKF),

*Corresponding author

which offers the advantage of explicitly modeling the stochastic uncertainties associated with the heart motion estimation and the straightforward fusion of external signals such as the ECG for improved prediction quality. However, the previous formulation was not capable of predicting the heart motion for larger prediction horizons, as needed in case of occlusions by surgical instruments. In this section, we present an improved motion model based on a time-varying dual Fourier series that explicitly models the cardiac and respiratory components that comprise the heart motion. Details of the design of the predictive EKF are given. Secondly, we show the improvements in visual tracking using the proposed prediction method for overcoming tracking disturbances and automatically reestablish tracking in case of occlusions. For designing and testing the motion prediction scheme, we use *in vivo* porcine beating heart motion data.

B. Beating heart motion dynamics

Here we present the key characteristics of the heart motion. High-speed images are necessary to properly capture the heart dynamics [7] and since the acquisition speed in commercial stereoscopes is limited, we used two high speed 1M75 DALSA cameras attached to Storz endoscopes mounted with a small baseline to simulate a real stereoscope. The system was calibrated using standard techniques [15]. Figure 1 displays the y trajectory of a POI on the surface of a porcine heart, acquired at 83.3 Hz using artificial markers attached to the heart surface. The acquisition setup is illustrated in figure 1. The heart was imaged for 60 seconds in an open chest configuration with no mechanical stabilization, which yields a heart motion amplitude considerably larger than in the MIS scenario. A frequency analysis shows that the dominant frequencies are situated between 0 - 2Hz, with significant energy up to 5Hz. These observations match similar experimental data reported in [2]. Also from the FFT plot, the two dominant frequencies associated to the respiratory and cardiac motions can be easily detected (the peaks corresponding to the harmonics of the two fundamental frequencies are highlighted).

C. Non-stationary dual Fourier series model

The heart motion can be considered as the sum of the respiratory and cardiac motions, which can be represented as a dual non-stationary Fourier series. Given the 3D coordinates $\mathbf{d} = [x \ y \ z]$ of a POI on the heart surface, the motion dynamics d of each Cartesian coordinate at a given instant t can be parameterized as:

$$d(t, \mathbf{f}) = \sum_{h=1}^{H_r} \left[a_h \sin \left(h \sum_{k=0}^t \omega_r(k) \right) + b_h \cos \left(h \sum_{k=0}^t \omega_r(k) \right) \right] + c_r + \sum_{h=1}^{H_c} \left[d_h \sin \left(h \sum_{k=0}^t \omega_c(k) \right) + e_h \cos \left(h \sum_{k=0}^t \omega_c(k) \right) \right], \quad (1)$$

where H_r and H_c are the number of harmonics for modeling the respiratory and cardiac components respectively, ω_r and ω_c are the respiratory and cardiac frequencies and

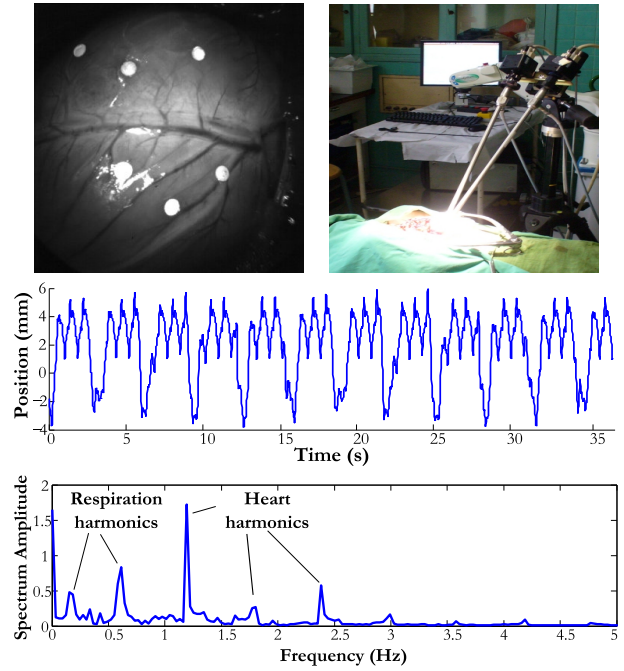


Fig. 1. **Heart Dynamics** (Top left) Markers used to retrieve the beating heart motion (Top right) *In vivo* experiment setup (Middle) y motion of a POI on the heart (Bottom) FFT spectrum of the y coordinate motion. The main peaks corresponding to the respiratory and cardiac harmonics are highlighted.

$\mathbf{f} = [a_1, \dots, a_{H_r}, b_1, \dots, b_{H_r}, c_r, d_1, \dots, d_{H_c}, e_1, \dots, e_{H_c}]$ is a vector containing the series coefficients. Note that the number of harmonics H_r and H_c among the $x \ y \ z$ directions may vary due to differences in their motion complexity. Finally, a POI has $n = 3 \cdot [2 \cdot ({}^x H_r + {}^x H_c) + 1 + 2 \cdot ({}^y H_r + {}^y H_c) + 1 + 2 \cdot ({}^z H_r + {}^z H_c) + 1]$ parameters plus the respiratory and cardiac frequencies, which are shared among coordinates. At a given instant t , the computation of q -step future position estimates using eq. (1) is done by assuming the system is stationary within the prediction horizon.

D. The Extended Kalman Filter

In our formulation, we employ the Kalman Filter (KF) for the recursive estimation of the Fourier series parameters. The KF offers several advantages, such as explicit modeling of the uncertainties associated with the proposed motion model and position measurements. Since estimating the Fourier series parameters is a nonlinear problem, the EKF is used [11].

The EKF state vector \mathbf{x} for estimating the trajectory of p POIs is composed $(p \cdot n + 2)$ parameters, where n is the number of parameters of the Fourier series. It is composed of the Fourier parameters $[\mathbf{f}_x, \mathbf{f}_y, \mathbf{f}_z]$ for the Cartesian coordinates of all estimated POIs and the cardiac and respiratory frequencies. When initializing the filter, no *a priori* knowledge of the signal is needed and all state vector values are set to zero except for the two frequencies, for which initial values (extracted from ECG and ventilation machine) are normally available in practice.

In the KF, estimation is divided between the prediction and correction phases. All parameters are modeled as random walk processes. In the prediction phase, the *a priori* estimate of the filter state \mathbf{x}^- at an instant k is given by the state values from the previous instant $k-1$. This implies that the error covariance matrix \mathbf{P} is propagated according to:

$$\mathbf{P}^-(k) = \mathbf{P}(k-1) + \mathbf{Q} \quad (2)$$

where \mathbf{Q} is the process covariance matrix. When initializing the filter, we use a process variance related to the respiratory components $\sigma_r^2 = 10^{-5}$ (with a variance $\sigma_c^2 = 10^{-6}$ for the offset c_r), the cardiac components $\sigma_c^2 = 10^{-5}$ and the frequencies variance $\sigma_w^2 = 10^{-8}$.

In the correction phase, the available measurements from the visual tracking algorithm \mathbf{y} are used to update the initial estimates \mathbf{x}^- , yielding the *a posteriori* estimate \mathbf{x}^+ . Notice that the tracking input \mathbf{y} is not filtered and therefore no delays are introduced in the system. The updated state is computed as:

$$\mathbf{x}^+(k) = \mathbf{x}^-(k) + \underbrace{\mathbf{P}^-(k)\mathbf{C}^T(k)(\mathbf{C}(k)\mathbf{P}^-(k)\mathbf{C}^T(k) + \mathbf{R})^{-1}}_{\mathbf{K}(k)}(\mathbf{y}(k) - d(k, \mathbf{x}^-(k))) \quad (3)$$

where \mathbf{R} is a diagonal matrix containing the measurement error covariance (the diagonal elements are set to 10^{-1}) and $\mathbf{C}(k)$ is a Jacobian matrix whose lines contain the derivatives of each motion component (as in equation 1) with respect to the Fourier series parameters. The matrix $\mathbf{K}(k)$ indicated above in equation 3 is the Kalman gain matrix. As an example, if we were to estimate only the x component of one POI, the matrix $\mathbf{C}(k)$ would be a $1 \times (^xH_r + ^xH_c + 2)$ matrix computed as:

$$\mathbf{C}(k) = \left. \frac{\partial d(t, \mathbf{x}_k)}{\partial \mathbf{x}_k} \right|_{\mathbf{x}_k = \hat{\mathbf{x}}_{k|k-1}} \quad (4)$$

The updated error covariance matrix is given by:

$$\mathbf{P}^+(k) = (\mathbf{I} - \mathbf{K}(k)\mathbf{C}(k))\mathbf{P}^-(k) \quad (5)$$

where \mathbf{I} is the identity matrix.

II. EXPERIMENTAL RESULTS

A. Predictive filter performance

For evaluating the performance of the proposed prediction method, we use the experimental data presented in section I-B. As stated in section I-C, predictions are computed using eq. (1), considering a stationary system within the prediction horizon. This idea is illustrated in figure 2, featuring the estimated Fourier series at an instant t_0 . Since motion is estimated on-line with all parameters initialized with zeros, 1.5 respiratory cycle (~ 400 samples) is needed for the model's parameters to converge. The number of harmonics for modeling respiration H_r for the xyz directions was set to 3, while for the cardiac motion $H_c = 5$ harmonics were sufficient.

For investigating the prediction performance in time, we evaluate the prediction error at every instant for 15, 83 and

TABLE I
PREDICTIVE FILTER PERFORMANCE ON *in vivo* DATA

Horizon	average RMS error (mm)	average peak error (mm)
0.18 s	0.8076	1.1829
1 s	0.8785	1.6764
3 s	1.0209	2.0496

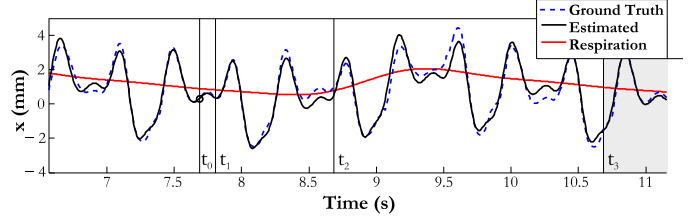


Fig. 2. Ground truth and estimated Fourier series at an instant t_0 . For evaluating prediction performance, we measure the prediction error for a 15, 83 and 250-step horizon prediction (0.18, 1 second and 3 seconds respectively).

250-step prediction horizons (0.18, 1 second and 3 seconds respectively). The error is calculated as the Euclidean distance $\|\mathbf{d} - \mathbf{p}\|$ between the predicted \mathbf{d} and true \mathbf{p} positions of the POI for all xyz coordinates. The root mean square and peak prediction errors at every motion sample for a given prediction horizon are measured. The prediction errors are plotted in figure 3 and quantified in table I. The identification error, which is the difference between the true position and the position estimated by the filter at a given instant is also plotted in figure 3.

The prediction filter must be robust to changes in the heart rhythm. In order to investigate the filter's behavior to amplitude changes, we slowly damp the original heart motion signal with respect to its mean to 50% of its original value in all Cartesian coordinates and analyze the behavior of the filter and the evolution of the prediction errors for a 1 second prediction horizon. Results are plotted in figure 4. Cardiac arrhythmia may also cause irregular heart motion and in order to analyze the filter's performance under such circumstances, we have simulated a disturbance in the heart-cycle in all Cartesian coordinates as illustrated in figure 5. The effects on the prediction error for a 1 second prediction horizon is plotted in figure 5.

B. Improvements in visual tracking

For evaluating the improvements in visual tracking, we use images of a porcine beating heart acquired using the same experimental setup presented in section I-B. For tracking the beating heart, we use the method described in [9] (the extension to other tracking methods such as [12] is straightforward).

The tracking method is based on a Thin-Plate Spline (TPS) function that models the heart tissue deformation. Tracking consists in the estimating the optimal TPS parameter vector \mathbf{h} that minimizes the alignment error between a manually chosen reference image \mathcal{T} and both left and right images

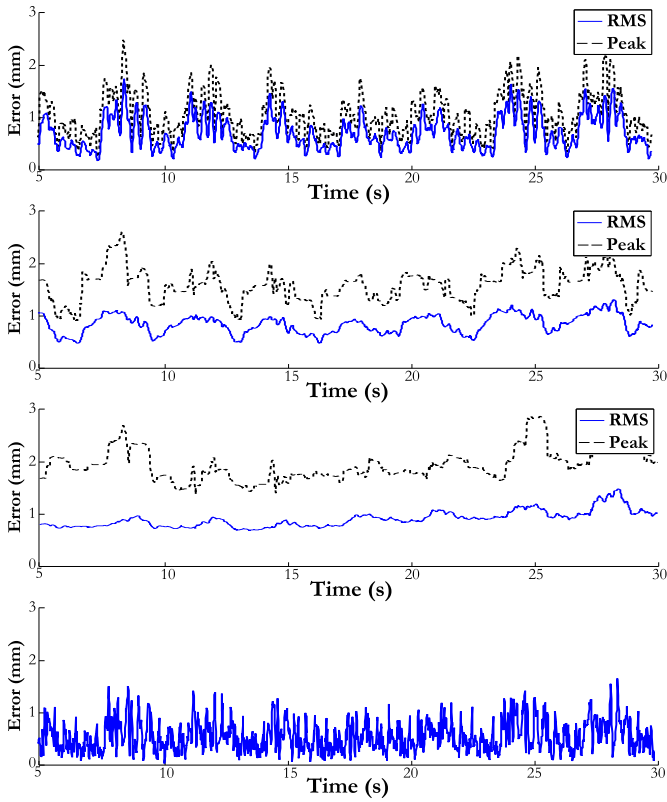


Fig. 3. From top to bottom, the RMS and peak prediction errors for a 15-step, 83-step, 250-step prediction horizon and the identification error, respectively.

of the stereo pair \mathcal{I}_l and \mathcal{I}_r simultaneously. The parameter vector \mathbf{h} is composed of 3D points that projects on both stereo cameras and therefore each point can be considered as a POI in the prediction framework presented before. Figure 6 displays a 128×128 pixel ROI on the heart tracked using the proposed method, using 6 control points for modeling the heart surface deformation.

1) *Specular reflections*: Specular reflections are the direct reflection of the illumination source on the glossy, wet-like heart surface. Such reflections saturate the affected pixels, disturbing considerably the visual tracking task. Figure 7 illustrates a case of tracking under such phenomenon. Although the tracking method automatically removes the affected regions from the estimation of the warping parameters, certain control points of the TPS mesh whose support region on the image is more severely affected by this phenomenon may be poorly estimated. In addition, depending on the duration of the perturbation, the estimation of the warping parameters may get stuck in local minima and diverge.

In the motion prediction context, specular reflections can be considered as occluders since no texture information is available from the affected areas. If the area affected by specular reflections goes beyond a critical level, tracking is suspended. In this context, the predicted heart motion can be used to bridge such disturbances, which normally last for approximately 0.12 s (15 frames in the acquisition speed

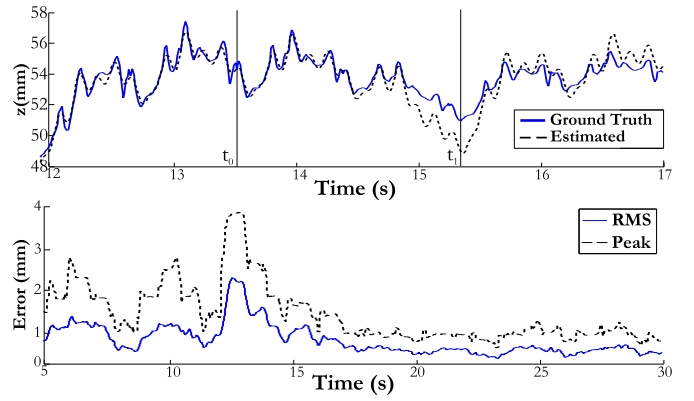


Fig. 4. (Top) The original heart motion is slowly damped from t_0 to t_1 to 50% of its original amplitude in all coordinates (due to space limitations only the z coordinate is illustrated). The dashed line shows the predicted heart motion at t_0 . (Bottom) The prediction error plot for a 1 second prediction horizon indicates the fast filter adaptation to the amplitude change. The RMS and peak errors are computed as in figure 3, considering all Cartesian coordinates. The time scale is increased for displaying the settling time.

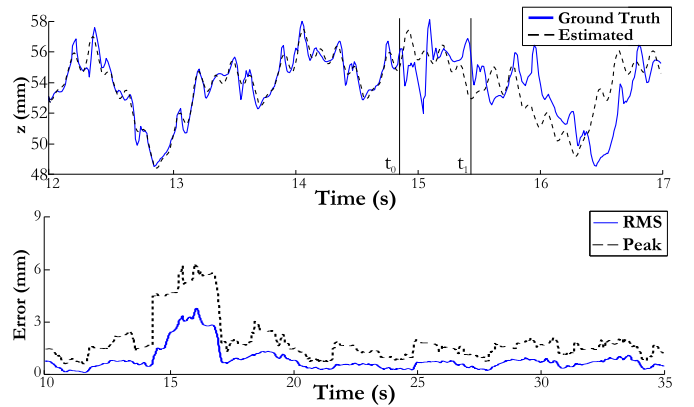


Fig. 5. (Top) A signal disturbance that resembles an arrhythmia is induced from t_0 to t_1 in all coordinates (due to space limitations only the z coordinate is illustrated). The dashed line shows the predicted heart motion at t_0 . (Bottom) The prediction error plots for a 1 second horizon indicate high prediction errors during the disturbance but the prediction quality is quickly reestablished past the disturbance. The RMS and peak errors are computed as in figure 3, considering all Cartesian coordinates. The time scale is increased for displaying the settling time.

used for the experiments).

2) *Occlusions*: The proposed motion prediction method also allows us to tackle the problem of occlusion by surgical tools. Surgical instruments eventually occlude the operating site for considerably longer periods of time and the proposed prediction scheme offers a solution for automatic tracking reinitialization in such cases.

In figure 8, the result of a simulated 3-second occlusion is presented, displaying the successful tracking reestablishment after the event. For simulating the occlusion, the correction step of the Kalman filter is suspended at an arbitrary instant t_0 and the predicted heart motion at t_1 3 seconds later was used to reestablish tracking. For visualizing the accuracy of the predicted heart motion, tracking results (the motion plots of one TPS control point) are also presented throughout

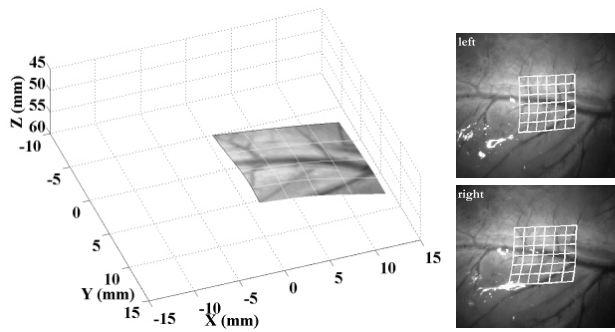


Fig. 6. (Left) The white mesh represents the TPS surface that models a selected ROI on the heart. (Right) The 3D shape of a ROI on the heart surface.

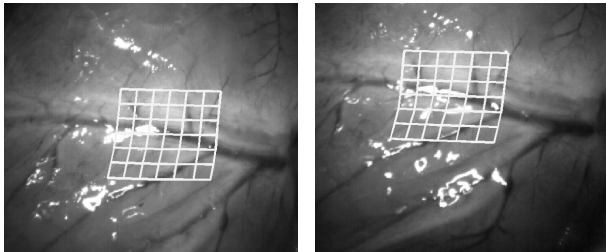


Fig. 7. The endoscopic illumination source reflects on the wet-like surface of the heart, giving rise to specular reflections that considerably disturb visual tracking.

the whole sequence for comparison purposes. An important remark after a visual inspection of the results is that although the predicted motion is accurate enough to restart tracking, it cannot be used for motion compensation since the prediction errors are superior than the precision required for performing the surgical gesture (which is under $200\mu\text{m}$).

C. Discussion of the predictive filter performance

The prediction errors presented in figure 3 reveal the good performance of the predictive filter, successfully acquiring the true heart dynamics. In addition, the error values given in table I indicate that the RMS and peak errors do not increase significantly when the prediction horizon is extended, suggesting the proposed motion model fits properly the heart motion. If the prediction horizon is further expanded, the prediction quality gradually degrades, due specially to small cardiac frequency variations.

The capacity of the filter to adapt to amplitude variations was properly displayed by the extreme simulation presented in figure 4. From the error plots, we can verify that the filter takes approximately 1s to re-adapt to the signal changes, later stabilizing in a lower level since the signal's amplitude was reduced by 50%.

Next, the simulated arrhythmic heart behavior presented in figure 5 is the most challenging event for the prediction filter. In fact, if we analyze the filter parameters in detail we learn that the abnormal heart behavior is interpreted as a drastic phase change. Although the error plots show a considerable large error during the event, the filter successfully copes with

the disturbance, converging quickly past the event. It is also important to remark that although the simulated arrhythmia generates a major disturbance in the predictive filter, such abnormal heart behavior can be easily detected from the heart electric activity and in practice it do not represent a critical problem.

Moreover, the relatively high identification error indicates that the heart motion model describes the coarse heart trajectory. This is due to the natural variability of the heart motion, since an increase of the number of harmonics does not lower this error. In fact, the number of harmonics is chosen according to the heart motion complexity and for the heart motion data used in the experiments, an increase of its number does not improve the performance.

The performance increase obtained with a Kalman filtering framework has been analyzed in previous works [14]. However, the direct comparison with experimental results of similar techniques proposed in the literature is not possible since the used experimental database highly influences the prediction errors, as clearly demonstrated when analyzing the amplitude changes in the input signal shown in the experimental section. This is due to the non linearity of the RMS error measure and the fact that the error amplitude is dependent on the amplitude of the heart motion.

The heart motion prediction can be further improved using the proposed formulation by exploring the ECG and respiratory signals directly in the filter design, as suggested in section I-D. For instance, the heart electric activity precedes the mechanical motion and the ECG waves may help predict more accurately the heartbeat contraction and relaxation cycles. The EKF framework adopted in this paper provides an elegant framework for fusing different sources of information in a straightforward fashion. Furthermore, the ECG can also be used for detecting abnormal cardiac behavior (e.g. arrhythmia). Another aspect of Kalman filtering is the adequate choice for the filter's covariance matrices. Although the values proposed in section I-D were not "fine" tuned for the experimental database, an adaptive update of the filter's uncertainty parameters could better estimate the heart motion, hence producing better future estimates. Finally, an increase of the number of harmonics does not significantly improve the prediction quality. Therefore, their number is kept small for avoiding unnecessary computations and possible convergence problems.

III. CONCLUSION

In this paper we proposed a new method for predicting the beating heart motion based on a time-varying dual Fourier series model whose parameters are estimated by an Extended Kalman filter. The proposed prediction method is applied in a visual tracking task with satisfactory results, successfully bridging tracking disturbances and reestablishing tracking in case of occlusions.

Direct applications of the proposed method can be found in other levels of the surgical robotic assistant such as the robot controller scheme. Currently, we are working on the

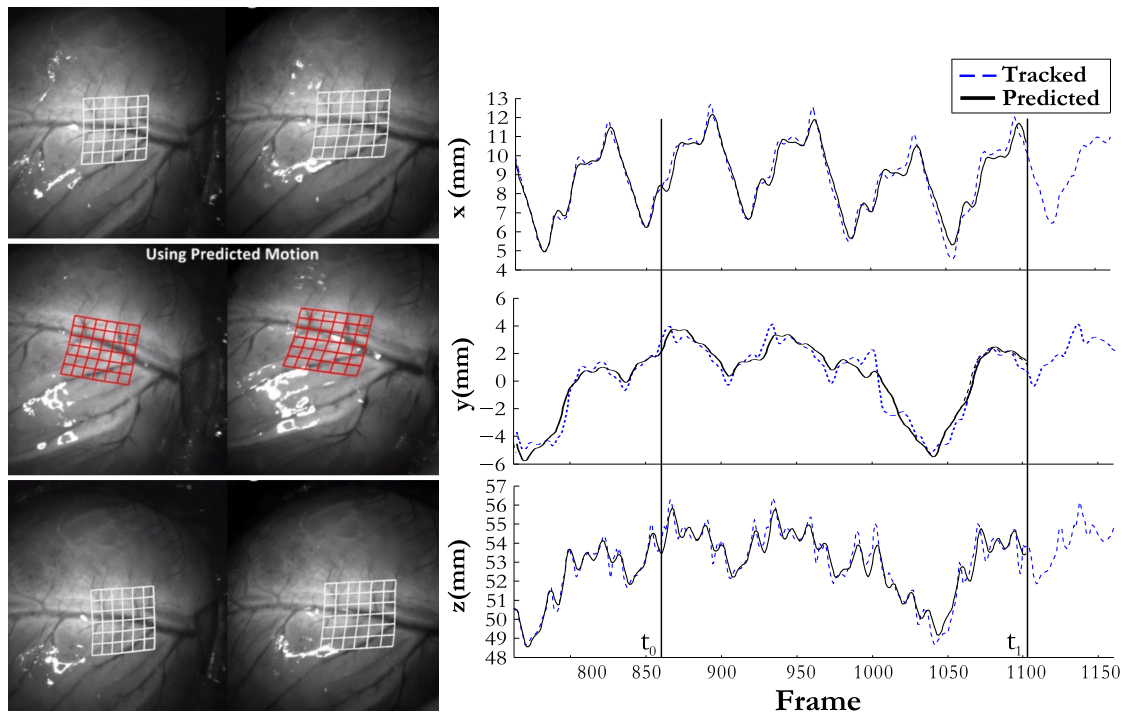


Fig. 8. (Left Top) The mesh illustrates the tracked region of interest on both left and right endoscopic images. (Left Middle) During the simulated occlusion, tracking is suspended and the predicted trajectory of the several POI that comprise the mesh is displayed as the mesh in red. (Left Bottom) Tracking is successfully reestablished past the occlusion. (Right) The predicted and tracked heart motion at an instant t_0 for the each Cartesian coordinate of a given POI in the tracked region.

incorporation of the proposed method in a model predictive controller for reducing the robot tracking error.

IV. ACKNOWLEDGEMENTS

This work is supported by the AccuRobAs project, under the 6th Framework Program (FP6) of the European Union. The authors would also like to thank the reviewers for their valuable comments.

REFERENCES

- [1] T. Bader, A. Wiedermann, K. Roberts, and U. D. Hanebeck, "Model-based motion estimation of elastic surfaces for minimally invasive cardiac surgery," in *Proceedings of IEEE Conference on Intelligent Robots and Systems (IROS '07)*, San Diego, USA, 2007, pp. 871–876.
- [2] O. Bebek and M. C. Cavusoglu, "Intelligent control algorithms for robotic-assisted beating heart surgery," *IEEE Transactions on Robotics*, vol. 23, no. 3, pp. 468–480, June 2007.
- [3] M. C. Cavusoglu, J. Rotella, W. S. Newman, S. Choi, J. Ustin, and S. S. Sastry, "Control algorithms for active relative motion cancelling for robotic assisted off-pump coronary artery bypass graft surgery," in *Proceedings of the 12th International Conference on Advanced Robotics (ICAR)*, Seattle, USA, 2005, pp. 431–436.
- [4] L. Cuvillon, "Compensation du battement cardiaque en chirurgie robotisée: Asservissement visuel d'un robot médical avec flexibilités," Ph.D. dissertation, Université Louis Pasteur - Strasbourg I, 2008.
- [5] V. Duindam and S. Sastry, "Geometric motion estimation and control for robotic-assisted beating-heart surgery," in *Proceedings of IEEE Conference on Intelligent Robots and Systems (IROS '07)*, San Diego, USA, 2007, pp. 871–876.
- [6] T. J. Franke, O. Bebek, and M. C. Cavusoglu, "Prediction of heart beat motion with a generalized adaptive filter," in *Proceedings of IEEE Conference on Robotics and Automation (ICRA '08)*, Pasadena, USA, 2008, pp. 2916–2921.
- [7] R. Ginhoux, J. Gangloff, M. de Mathelin, L. Soler, M. A. Sanchez, and J. Marescaux, "Active filtering of physiological motion in robotized surgery using predictive control," *IEEE Transactions on Robotics*, vol. 21, no. 1, pp. 67–79, February 2003.
- [8] T. Ortmaier, M. Groger, D. H. Boehm, V. Falk, and G. Hirzinger, "Motion estimation in beating heart surgery," *IEEE Transactions on Biomedical Engineering*, vol. 52, no. 10, pp. 1729–1740, 2005.
- [9] R. Richa, A. P. L. Bó, and P. Pognet, "Motion prediction for tracking the beating heart," in *Proceedings of IEEE International Conference of the Engineering in Medicine and Biology Society (EMBS '08)*, Vancouver, Canada, 2008, pp. 3261–3264.
- [10] R. Richa, P. Pognet, and C. Liu, "Efficient 3d tracking for motion compensation in beating heart surgery," in *Medical Image Computing and Computer-Assisted Intervention (MICCAI '08)*, ser. Lecture Notes in Computer Science (LNCS). New York, USA: Springer, 2008, pp. 684–691.
- [11] D. Simon, *Optimal State Estimation: Kalman, "H_∞" and Nonlinear Approaches*. John Wiley & Sons, Inc., 2006.
- [12] D. Stoyanov, G. P. Mylonas, F. Deligianni, A. Darzi, and G. Z. Yang, "Soft-tissue motion tracking and structure estimation for robotic assisted mis procedures," in *Medical Image Computing and Computer-Assisted Intervention (MICCAI '05)*, ser. Lecture Notes in Computer Science (LNCS), vol. 3750. Palm Springs, USA: Springer, 2005, pp. 139–146.
- [13] A. Thakral, J. Wallace, D. Tomlin, N. Seth, and N. V. Thakor, "Surgical motion adaptive robotic technology (s.m.a.r.t): Taking the motion out of physiological motion," in *Medical Image Computing and Computer-Assisted Intervention (MICCAI '01)*, ser. Lecture Notes in Computer Science (LNCS). Utrecht, The Netherlands: Springer, 2001, pp. 317–325.
- [14] S. G. Yuen, P. M. Novotny, and R. D. Howe, "Quasiperiodic predictive filtering for robot-assisted beating heart surgery," in *Proceedings of IEEE Conference on Robotics and Automation (ICRA '08)*, Pasadena, USA, 2008, pp. 1050–1059.
- [15] Z. Zhang, "A flexible new technique for camera calibration," *IEEE Transactions on Pattern Analysis and Machine Intelligence (PAMI)*, vol. 22, no. 11, pp. 1330–1334, 2000.